A new Schiff base derivative based on the ratiometric fluorescent chemosensor for detection of Mg^{2+} ions and Spectroscopy applications

Pitchai Marimuthu
Madurai Kamaraj University
Andy Ramu (andyramumku@gmail.com)
Madurai Kamaraj University

Research Article

Keywords: Interaction with 8-HQC-2TCH to Mg2+ ion

Posted Date: May 11th, 2022

DOI: https://doi.org/10.21203/rs.3.rs-1611320/v1

Abstract

A novel ratiometric fluorescence sensor, (E)-N'-((8-hydroxyquinolin-2-yl) methylene) thiophene-2-carbohydrazide has been constructed for the selective and sensitive detection of Mg^{2+} ion. Fluorescence sensing of Mg^{2+} is highly solvent as well as imine structure dependent. It showed a significant fluorescence ratiometric towards Mg^{2+}ions. The receptor 8-HQC-2TCH exhibited a good binding constant and lowest detection limit for Mg^{2+}. These phenomena result from the rapid coordination between Mg^{2+} and 8-HQC-2TCH in the presence of Mg^{2+}, which leads to the theoretical ratiometric of the fluorescence of probe. On the basis of these findings, ratiometric fluorescence sensor for the detection of Mg^{2+} ion reveals a good linear response to Mg^{2+} ranging from 0 to 60 mM with a detection limit of 3.9×10^{-7} M. Furthermore, the sensing assay is applicable to detecting Mg^{2+} in real samples.

Introduction

Many chemistry, biologists and medical & pharmaceutical have attracted towards the design and development of highly sensitive fluorescent probes, for the detection of various metal ions in environmental and biological systems. [1-3] Magnesium is the major indispensable metals due to its capability to mediate in many enzyme-catalyzed reactions in biochemists of in addition humans [4-6], these elements have an important role in regulating a wide variety of physiological and pathological processes [7]. Magnesium is found in the bones as macronutrient, and involved in the bone remodelling skeletal development [8,9]. Magnesium deficiency has caused number of chronic diseases, such as osteoporosis, hypertension, coronary heart disease, and diabetes [10-12]. Magnesium research has aroused its importance in clinical medicine, especially for the of nutrition and physiology [13,14], however, when compared with the other metal ions [15-17], only few reports exists address Mg^{2+} . In general, fluorescence probes, has limited their practical usage in low sensitivity and selectivity [18,19] and higher detection limits [20,21]. The main principles behind sensing mechanisms are intramolecular charge transfer (ICT), photo induced electron transfer (PET), intermolecular hydrogen bonding, and fluorescence resonance energy transfer [22-27]. Ratiometric sensing is highly preferred in which higher accuracy in quantity analytes needed [28]. Aprotic solvent with high selectivity is desirable for the design and synthesis of probes for Mg^{2+} detection [29-34]. In this reaction, Schiff-bases nitrogen–oxygen-rich coordination [35-39], fluorescence group will probably emit fluorescence in the presence of metal ions is selective feasible to design and develop a fluorescent probe [40-43].

Chemical Sensors

A chemical sensor is a device that transforms chemical information, ranging from the concentration of a specific sample component to the total composition analysis, into an analytically useful signal. [50]

Especially quinoline derivative in which higher accuracy in quantity analytes needed. Hence, Schiff base with of 8-hydroxyquinoline-2-carboxaldehyde moiety has been report for development of a turn-on fluorescent responsive molecular sensor for Mg^{2+}. The probe was characterized by ESI-MS and NMR

techniques. The fluorescence experiments of selected metal ions display a dramatic fluorescence intensity enhancement for Mg^{2+} over all other cations were carried out at the explore results 8-HQC-2TCH is a suitable probe to sense Mg^{2+} ion. Binding mechanism of 8-HQC-2TCH +Mg^{2+} was also studied by using DFT.

Results And Discussion

Characterizations UV-vis spectral studies

The absorption of 8-HQC-2TCH towards different metal cations was investigated by adding of Al^{3+}, Cd^{2+}, Co^{2+}, Cu^{2+}, Fe^{3+}, Hg^{2+}, Mg^{2+}, Mn^{2+}, Ni^{2+}, Pb^{2+}, Zn^{2+} in DMSO as their metal salts. To being with, the 8-HQC-2TCH was characterized by UV-Visible absorption Spectroscopy and the observed results are shown in (**Fig. 4A**). The UV-visible spectrum displays 8-HQC-2TCH absorption band 300 nm could attribute to π-π* transitions. The Mg^{2+} ion was significant to be a new absorption band at 430 nm. Quantitatively shifted in direction to check the sensitivity of the 8-HQC-2TCH towards Mg^{2+} ion, the sensitivity investigates were also performed by the addition of several concentrations of Mg^{2+} ions. Absorption bands at 430 nm are slowly increased with may be due to the formation of the complex (**Fig. 4B**).

The absorption spectrum of 8-HQC-2TCH was recorded in the range of 0-60 mM of $Mg^{2+}$and observed the detection limit 3.6 $x10^{-7}$ M for Mg^{2+} ion by using the absorbance titration data. The competitive studies of HQC-2TCH for Mg^{2+} in the presence of other metal ions revealed that Al^{3+}, Cd^{2+}, Hg^{2+} Cr^{3+}, Fe^{3+}, Mn^{2+}, Co^{2+}, Ni^{2+} and Cu^{2+} had negligible interference. But no turn-on fluorescence was observed for Mg^{2+} in the presence of Transition metal ions, showed a strong influence on the Mg^{2+} selectivity that could be due to the stronger coordination with HQC-2TCH (see **Figure. S5-6**).

Fluorescence analysis of 8-HQC-PTH detection of Mg^{2+}

The fluorescence spectra of compound 8-HQC-2TCH with its metal ions showed (**Fig.7A**). The emission band obtained from 8-HQC-2TCH was quite significant in the presence of Mg^{2+} ion. 8-HQC-2TCH showed fluorescence intensity at 480 nm and the new band appeared at 600 nm while upon addition of Mg^{2+} ion, confirm that the fluorescence intensity displays Mg^{2+} ions induced fluorescence changes, while other metal ions did not fluorescence changes, which clearly indicate, that the 8-HQC-2TCH has good selectivity towards Mg^{2+} ion over the additional competing cations.

Fluorescence spectroscopic titrations were also carried out under similar conditions to obtain a better insight into the response of 8-HQC-2PTCH towards Mg^{2+} ions. As shown in (**Fig. 7B**),when excited at 340 nm, the fluorescence band at 480 nm decreased and a band at 600 nm increased which provides ratiometric fluorescence spectra, and isoemittive point at 550 nm, when the gradually increasing the concentration of Mg^{2+} ion from 0 to 70 mM. Moreover, the quenching efficiency was analysed by following Stern-Volmer Eqn 2:

$F_0/F = K_{sv}[Q] + 1$…… (eqn. 2)

Where F_0 and F are the intensities of 8-HQC-2TCH before and also after the addition of Mg^{2+}, and [Q] is the molar concentration of the Mg^{2+} and K_{sv} is the quenching constant. The detection limit to be found 4.9×10^{-8} M for 8- HQC-2TCH. The binding constant 4.3 x10-3 M^{-1} accrues for the completed was (**Fig. 8A-8B**).

Competitive of 8-HQC-PTH

The fluorescence response of the sensing system towards Mg^{2+} ion in the presence of other metal ions was studied and the data were shown in (**Fig. 9**). The orang bars represent the fluorescence intensity of 8-HQC-2TCH with metal ions and the Cyan bar represents the fluorescence intensity of 8-HQC-2TCH + Mg^{2+} with other competing cations. The presence of the selected metal ion does not interfere with Mg^{2+} complex with the 8-HQC-2TCH, indicates that negligible interference effects on Mg^{2+} sensing were absent. The sensor 8- HQC-2TCH was effective to form a 1:1 complex, are confirmed by Job's plot analysis. This binding stoichiometric was further confirmed by ESI-MS (**Fig. 10-11**).

Intramolecular charge transition (ICT) mechanism has been proposed in this study under investigational conditions. The ICT from the electron-rich quinoline to hydrazide takes place (**Scheme 2**), when Mg^{2+} ion added, the charge transfer was arrested due to the strong complexation of Mg^{2+} with 8- HQC-2TCH. Though four coordination of Mg^{2+} ion with the hydroxyl of quinoline ring, the nitrogen of quinoline moiety (N), imine nitrogen (C=N) and the nitrogen (-NH) of hydrazide moiety was proposed. In addition, it is well known that Mg^{2+} ion (a Soft acid), differently interacts with the nitrogen, and hydroxyl group according to Pearson's HSAB theory. The modifications in the fluorescence spectrum, quenching intensity atb480 nm the new band at 600 nm were of Mg^{2+} ion, obviously justified.

Mechanism of Sensing Fluorometric Mg^{2+} ion

The proposed geometry of the probe (8-HQC-2TCH) was optimized using DFT-B3LYP 6-31G level using Gaussian 09 package. Binding sites of complex with Mg^{2+}, experimental finding supports Job's plot. DFT calculations, shows that the quinoline unit act as HOMO whereas thiophene unit act as LUMO of 8-HQC-PTH, indicating that the intramolecular charge transfer (ICT) slightly takes place from the quinoline unit to hydrazide unit.

The ICT is inhibited resulting in remarkable fluorescence quenching. For the Mg^{2+} complex the HOMO act as thiophene part and the electron density are found to spread over whole moiety at LUMO, which indicates restriction of the ICT process and fluorescence quenching is occurs. In addition, the energy gap between the HOMMO and LUMO of the chemosensor is higher than it's complex, this is clearly indicate that strong chelation occurred between the Mg^{2+} and chemosensor (**Fig. 12)**.

Table 1. Comparison table for various probes for the detection of Mg^{2+}.

S.N	8-HQC-2TCH	Metal	Detect limit	Application	Ref
1	Isatin-3-(7-Methoxychromone-3-methylidene) hydrazone	Mg^{2+}	5.16 x 10^{-7} M	Fluorescent “turn-on” sensor	45
2	4-hydroxy-3-((2-hydroxy-5-methylphenyl)diazenyl)-2H-chromen-2-one	Mg^{2+} & F^{-}	2.4 x 10^{-8} M & 2.3 x 10^{-8} M	Fluorescent “*turn-on-off*” sensor	46
3	N-(1H-benzo[d]imidazol-2-yl)quinoline-2-carboxamide (QLBM)	Cu^{2+}, Fe^{3+}	1.35× 10^{-7} M & 1.24 × 10^{-7} M	Fluorescent sensor and Live cell imaging	48
4	N-(quinolin-8-yl)-2-(quinolin-8-yloxy) acetamide	Zn^{2+} & Cd^{2+}	1.8 × 10^{-4} M & 1.9 x 10^{-7} M	Fluorescent “*turn-on*” sensor	47
5	2-Hydroxyquinoline-3-carbaldehyde	Zn^{2+} & Ni^{2+}	7.2 x 10^{-8} M & 3.3 x 10^{-7} M	Live cell imaging on lung cancer cell line	49
6	**(8-HQC-PTH)**	**Mg^{2+}**	**4.9 x 10^{-8} M**	**Ratiometric Fluorescent sensor**	**This work**

Conclusion

In conclusion, a highly selective and sensitive fluorescence chemosensor 8-HQC-2TCH molecule in DMSO solution for Mg^{2+} ion is reported. The 8-HQC-2TCH has been characterized by NMR and ESI-MS spectroscopy. The detection limit to be found 4.9 x 10^{-8} M for 8- HQC-2TCH. The sensing mechanism of this ratiometric chemosensor has been confirmed by using DFT and NMR titration analysis. 8-HQC-2TCH expresses a clear ICT mechanism and the later addition of the Mg^{2+} ions indicates the suppresses of ICT and a new band seen at 590 nm. This is used for selectivity and sensitivity experiments. All the spectroscopic experiments were results at room temperature.

Experimental

Materials and methods

All solvents and chemicals employed for synthesis were commercially available and purchased from Aldrich and Merck and used without further purification. The ligand 8-HQC-2TCH was synthesized by the benign method developed in our laboratory and characterized by different spectroscopic techniques. UV-Vis spectra were recorded on a JASCO-500 spectrophotometer with a quartz cuvette (cell length 1cm). The fluorescence spectra were recorded with an Agilent Cary Eclipse Fluorescence Spectrofluorimeter. ^{1}H and ^{13}C NMR spectra were recorded on a BRUKER 300 MHz spectrometer using $CDCl_3$ and DMSO-$d_6$as solvent using TMS as the internal standard. ESI-MS analysis was performed on the positive and negative ion modes on a liquid chromatography–ion-trap mass spectrometry instrument (LCQ Fleet, Thermo Fisher Instruments Limited, USA). DFT calculations were performed at the B3LYP/LANL2DZ (d) level using the Gaussian 09 program.

Determination of the limit of detection and binding constant

The foundation of the fluorescence titration curve of 8-HQC-2TCH with the addition of Mg^{2+} (0–70μM), the detection limit was acquired. The standard deviation of blank control was finalized when the fluorescence intensity of 8-HQC-2TCH was measured. The detection limit was determined by the following equation [44] 1:

Detection limit = $3\sigma_i/k$…… (eqn. 1)

Where σ_i is the standard deviation of the blank experiment, and k is the slope between the fluorescence ratios (I_{min}/I_{max}) versus Mg^{2+} concentration.

Preparation of Sensors solution

A sensing study of the solution of probe 8-HQC-2TCH (1 $x10^{-3}$)was prepared in DMSO solution. Metal ion solutions were prepared in the equal concentration using double distilled water. Standard solution of 8-HQC-2TCH (50 μL) was prepared diluted by using DMSO solvents (2 ml of DMSO to an absolute concentration of 25 μM),

Synthesis of probe (8-HQC-2TCH)

The 2-thiophene carboxylic acid hydrazide (0.034g, 1mmol) was slowly added to the 8-hydroxyquinoline-2-carbaldehyde (0.04 g, 1mmol) dissolved in ethanol solvents (15 ml). The reaction mixture was refluxed at 85°C for 6h. The progress of the reaction was monitored by thin layer chromatography and after completion of the reaction, the reaction mixture was cooled to 27 ^{0}C. A yellow solid was obtained with 85% yield.

As shown in (**Scheme 1)**, the reaction between 8-hydroxyquinoline-2-carbaldehyde and 2-thiophene carboxylic acid hydrazide produced a Schiff's base as a yellow solid with 85% yield, were fully characterized by NMR and ESI-Mass. The $^{1}H_{1}$ NMR, ^{13}C NMR, and ESI-Mass spectra are delivered in the (see **Figure. S1-3)**.

Declarations

Acknowledgements:

P. M. extends his acknowledgment to the School of Chemistry, Madurai Kamaraj University for providing adequate instrument facilities through DST-IRHPA, FIST, DST-PURSE, and UGC-UPE schemes.

Authors' Contributions:

All authors contributed in the present study. All authors commented on this version of the manuscript and they read and approved the final manuscript.

Funding:

The authors have no relevant financial or non-financial interests to disclose.

Data Availability:

All data contained in the current manuscript and supplementary information are available.

Conflict of interest: All authors declare no conflict of interest.

Ethics approval: Not applicable.

Consent to participate: Not applicable.

Consent to publish: Not applicable.

Supplementary information:

The complementary information about all experiments and theoretical calculations is included in the supplementary information.

References

1. Silva APD, Gunaratne HQN, Gunnlaugsson T, Huxley AJM, McCoy CP, Rademacher JT, Rice TE (1997) Signaling recognition events with fluorescent sensors and switches. Chem Rev 97:1515–1566
2. Sivaraman G, Anand T, Chellappa D (2012) Turn-on fluorescent chemosensor for Zn (II) via ring opening of rhodaminespirolactam and their live cell imaging. Analyst 137:5881–5884

3. Wu J, Liu W, Ge J, Zhang H, Wang P (2011) New sensing mechanisms for design of fluorescent chemosensors emerging in recent years. Chem Soc Rev 40:3483–3495
4. Murugan AS, Nelson ERA, Annaraj J (2016) Solvent dependent colorimetric, ratiometric dual sensor for copper and fluoride ions: Real sample analysis, cytotoxicity and computational studies. Inorg Chim Acta 450:131–139
5. Wang M, Zhang G, Zhang D, Zhu D, Tang BZ (2010) Fluorescent bio/ chemosensors based on silole and tetraphenylethene luminogens with aggregation-induced. J Mater Chem 20:1858–1867
6. Sivaraman G, Sathiyaraja V, Chellappa D (2014) Turn-on fluorogenic and chromogenic detection of Fe (III) and its application in living cell imaging. J Lumin 145:480–485
7. Kim KB, Kim H, Song EJ, Kim S, Noh I, Kim C (2013) A new multifunctional Schiff base as fluorescence sensor for Al^{3+} and colorimetric sensor for CN^{-} in aqueous media: an application to bioimaging. Dalton Trans 42:6650–6659
8. Wang J, Lin W, Li W (2012) Single fluorescent probe displays a distinct response to Zn^{2+} and Cd^{2+}. Chem Eur J 18:13629–13632
9. Liu X, Zhang N, Zhou J, Chang T, Fanga C, Shangguan D (2013) A turn-on fluorescent sensor for zinc and cadmium ions based on perylenetetra carboxylicdiimide. Analyst 138:901–906
10. Poinern GEJ, Brundavanam S, Fawcett D (2012) Biomedical magnesium alloys: a review of material properties, surface modifications and potential as a biodegradable orthopaedic implant. Am J Biomed Life Sci 2:218–240
11. Men G, Chen C, Zhang S, Liang C, Wang Y, Deng M, Shang H, Yang B, Jiang S (2015) A real-time fluorescent sensor specific to Mg^{2+} crystallographic evidence, DFT calculation and its use for quantitative determination of magnesium in drinking water. Dalton Trans 44:2755–2762
12. Jamshidi M, Rezaei O, Belverdi AR, Malekian S, Belverdi AR (2016) A highly selective fluorescent chemosensor for Mg^{2+} ion in aqueous solution using density function theory calculations. J Mol Struct 123:111–115
13. Yang MD, Zhang Y, Zhu WJ, Wang HZ, Huang J, Cheng LH, Zhou HP, Wu JY, Tian YP (2015) Difunctional chemosensor for Cu (II) and Zn (II) based on Schiff base modified anthryl derivative with aggregation-induced emission enhancement and piezochromic characteristic. J Mater Chem 3:1994–2002
14. Nugent JW, Lee H, Reibenspies JH, Lee H-S, Hancock RD (2017) Effects of anion coordination on the fluorescence of a photo-induced electron transfer (PET) sensor complexed with metal ions. Polyhedron 130:47–57
15. Wazzan N, Safi Z (2017) DFT calculations of the tautomerization and NLO properties of 5-amino-7-(pyrrolidin-1-yl)-2,4,4-trimethyl-1,4-dihydro-1,6-naphthyridine-8- arbonitrile (APNC). J Mol Struct 1143:397–404
16. An B, Yuan H, Zhu Q, Li Y, Guo X, Zhang J (2017) Theoretical insight into the excited-state intramolecular proton transfer mechanisms of three amino-type hydrogen-bonding molecules.

Spectrochim Acta A 36:36–42

17. Yuan S, Feng K, Wen Q, Zhu B, An X, Guo J, Zhang J (2017) A quantum-chemical insight into the tunable fluorescence color and distinct photoisomerization mechanisms between a novel ESIPT fluorophore and its protonated form. Spectrochim Acta A 183:123–130
18. Taherpour AA, Jamshidi M, Rezaei O (2017) Theoretical Studies on Photo-induced Electron Transfer Process on [Cefamandole] C_{60} Nano-Complex. J Mol Graph Model 75:42–48
19. Yeung MC-L, Yam VW-W (2015) Luminescent cation sensors: from host-guest chemistry, supramolecular chemistry to reaction-based mechanisms. Chem Soc Rev 44:4192–4202
20. Zhao L, Liu Y, He C, Wang J, Duan CY (2014) Synthesis and Characterization of a Mg^{2+} Selective Fluorescent Probe. Sensors 43:335–343
21. Maguire ME, Cowan JA (2002) Magnesium chemistry and biochemistry. Bio Met 15:203–210
22. Hariharan P, Anthony SP (2014) Selective fluorescence sensing of Mg^{2+} ions by Schiff base chemosensor: effect of diamine structural rigidity and solvent. RSC Adv 4:41565–41571
23. Dong Y, Li J, Jiang X, Song F, Cheng Y, Zhu C (2011) Na^{+} triggered fluorescence sensors for Mg^{2+} detection based on a coumarinsalen moiety. Org Lett 13:2252–2255
24. O'Rourke B, Backx PH, Marban E (1992) Phosphorylation-independent modulation of L-type calcium channels by magnesium-nucleotide complexes. Science 257:245–248
25. Schmitz C, Perraud A, Johnson CO, Inabe K, Smith MK, Penner R, Kurosaki T, Feig A, Scharenberg AM (2003) Regulation of vertebrate cellular Mg^{2+} homeostasis by TRPM7. Cell 114:191–200
26. Mann FM, Prisic S, Davenport EK, Determan MK, Coates RM, Peters RJ (2010) A Single Residue Switch for Mg^{2+}dependent Inhibition Characterizes Plant Class II DiterpeneCyclases from Primary and Secondary Metabolism. J Biol Chem 285:20558–20563
27. Farruggia G, Iotti S, Prodi L, Montalti M, Zaccheroni N, Savage PB, Trapani V, Sale P, Wolf FI (2006) 8-hydroxyquinoline derivatives as fluorescent sensors for magnesium in living cells. J Am Chem Soc 128:344–350
28. Kim HM, Yang PR, Seo MS, Yi J-S, Hong JH, Jeon S-J, Ko Y-G, Lee KJ, Cho BR (2007) Magnesium Ion selective two-photon fluorescent probe based on a benzo[h]chromene derivative for in vivo imaging. J Org Chem 72:2088–2096
29. Ajayaghosh A (2005) Chemistry of Squaraine-Derived Materials: Near-IR Dyes, Low band gap systems, and cation sensors. Acc Chem Res 38:449–459
30. Kim J, Morozumi T, Nakamura H (2007) New fluorescent "Off-On" behavior of 9-anthryl aromatic amides through controlling the twisted intramolecular charge transfer relaxation process by complexation with metal ions. Org Lett 9:2923–2931
31. Suzuki Y, Komatsu H, Ikeda T, Saito N, Araki S, Citterio D, Hisamoto H, Kitamura Y, Kubota T, Nakagawa J, Oka K, Suzuki K (2002) Design and synthesis of Mg^{2+}selective fluoroionophores based on a coumarin derivative and application for Mg^{2+} measurement in a living cell. Anal Chem 74:1423–1428

32. Ray D, Bharadwaj PK (2008) A Coumarin-derived fluorescence probe selective for magnesium. Inorg Chem 47:2252–2254
33. Kao MH, Chen TY, Cai YR, Hu C-H, Liu YW, Jhong Y, Wun AT (2016) A turn-on Schiff-base fluorescence sensor for Mg^{2+} ion and its practical application. J Lumin 169:156–160
34. Liu Y-W, Chen C-H, Wu A-T (2012) A turn-on and reversible fluorescence sensor for Al^{3+} ion. Analyst 137:5201–5203
35. Lu CY, Liu Y-W, Hung P-J, Wan CF, Wu AT (2013) Polynorburnene based sensor for “IN FIELD” heavy metal and nerve agent sensing application. Inorg Chem Commun 35:371–412
36. Chang Y-J, Hung P-J, Wan C-F, Wu A-T (2014) A highly selective fluorescence turn-on and reversible sensor for Al^{3+} ion. Inorg Chem Commun 39:122–125
37. Khan RI (2016) Pitchumani, β-Cyclodextrin Included Coumarin Derivatives as Selective Fluorescent Sensors for Cu^{2+} ions in HeLa Cells. RSC Adv 6:20269–20275
38. Murugan AS, Pandi M, Annaraj J, Single A (2017) Simple Receptor as a Multifunctional Chemosensor for the Al^{3+}/Cu^{2+} ions and Its Live Cell Imaging Applications. Chem Select 2:375–383
39. Adhikari S, Ghosh A, Guria S, Sarkar S, Sahana A (2016) Naturally occurring thymol based fluorescent probes for detection of intracellular free Mg^{2+} ion. Sens Actuators B 236:512–519
40. Gharami S, Sarkar D, Ghosh P, Acharyya S, Aich K, Murmu N, Mondal TK (2017) A coumarin based azo-phenol ligand as efficient fluorescent “OFF-ON-OFF” chemosensor for sequential detection of Mg^{2+} and F^{-} Application in live cell imaging and as molecular logic gate. Sens Actuators B 253:317–325
41. Wang G-Q, Qin J-C, Fan L, Li C-R, Yang Z-Y (2016) A turn-on fluorescent sensor for highly selective recognition of Mg^{2+} based on new Schiff’s base derivative. J Photochem Photobiol A 314:29–34
42. Yu C, Fu Q, Zhang J (2014) Synthesis and characterization of a Mg^{2+} selective fluorescent probe. Sensors 14:12560–12567
43. Taherpour AA, Jamshidi M, Rezaei O (2017) Recognition of Switching On or Off fluorescence emission spectrum on the schiff-bases as a Mg^{2+} chemosensor: a first principle DFT and TD-DFT. J Mol Struct 1147:815–820
44. Zhou X, Li P, Shi Z, Tang X, Chen C, Liu W (2012) A highly selective fluorescent sensor for distinguishing cadmium from Zinc ions based on a quinoline platform. Inorg Chem 51:9226–9231
45. Zhang B, Liu H, Wu F, Hao G, Chen Y, Tan C, Tan Y, Jiang Y (2017) A dual-response quinoline-based fluorescent sensor for the detection of Copper (II) and Iron (III) ions in aqueous medium. Sens Actuators B 243:765–774
46. Kim H, Kang J, Kim KB, Song EJ, Kim C (2014) A highly selective quinoline-based fluorescent sensor for Zn(II). Spectrochim Acta A 118:883–887
47. Tian J, Yan X, Yang H, Tian F (2015) A novel turn-on Schiff-base fluorescent sensor for aluminum (III) ions in living cells. RSC Adv 5:107012–107019

48. Murugan AS, Vidhyalakshmi N, Ramesh U, Annaraj J (2017) A Schiff's base receptor for red fluorescence live cell imaging of Zn^{2+} ions in zebrafish embryos and naked eye detection of Ni^{2+} ions for bio-analytical application. J Mater Chem B 5:3195–3200
49. Zhao Q, Yu M, Shi L, Liu S, Li C, Shi M, Zhou Z, Huang C, Li F (2010) Cationic iridium(III) complexes with tunable emission colour as phosphorescent dyes for live cell imaging. Organometallics 5:1085–1091
50. Geab AHS (1991) F I Pure Appl Chem 63:1247–1250.

Scheme

Scheme 1 is not available with this version

Scheme 2 is available in supplementary section.

Figures

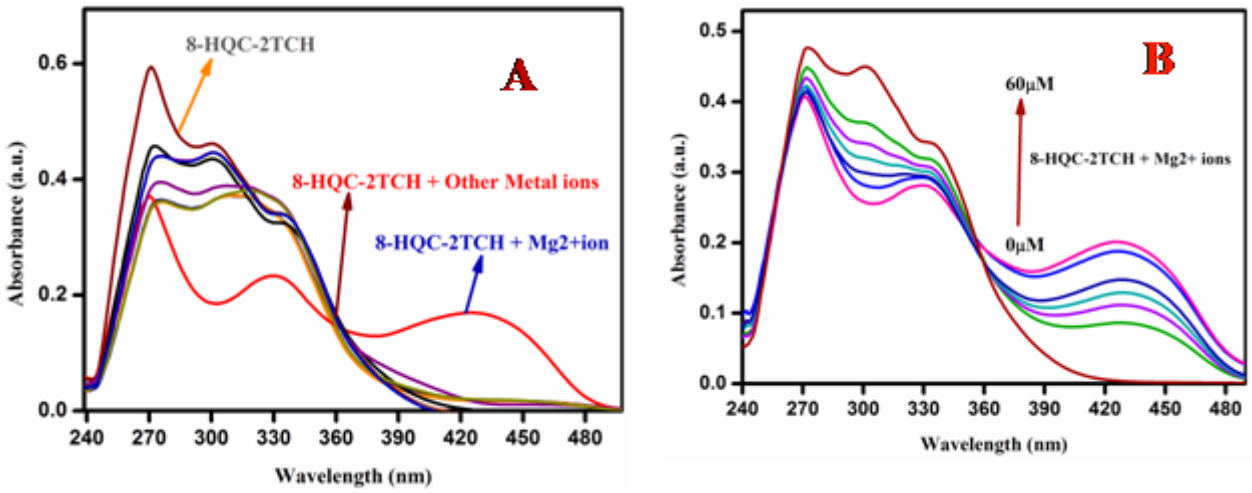

Figure 1

Figure 4A. UV–Vis. Spectra of 8-HQC-2TCH (25 μM) in the presence of various metal ions such as K^{+}, Mg^{2+}, Ba^{2+}, Cu^{2+}, Al^{3+}, Fe^{3+}, Zn^{2+}, Cd^{2+}, Hg^{2+} and Cr^{3+} (25 μM) in DMSO. **B.** UV–Vis. Spectra of 8-HQC-2TCH (25 μM) upon the titration of Mg^{2+} 0 to 60 mM in DMSO.

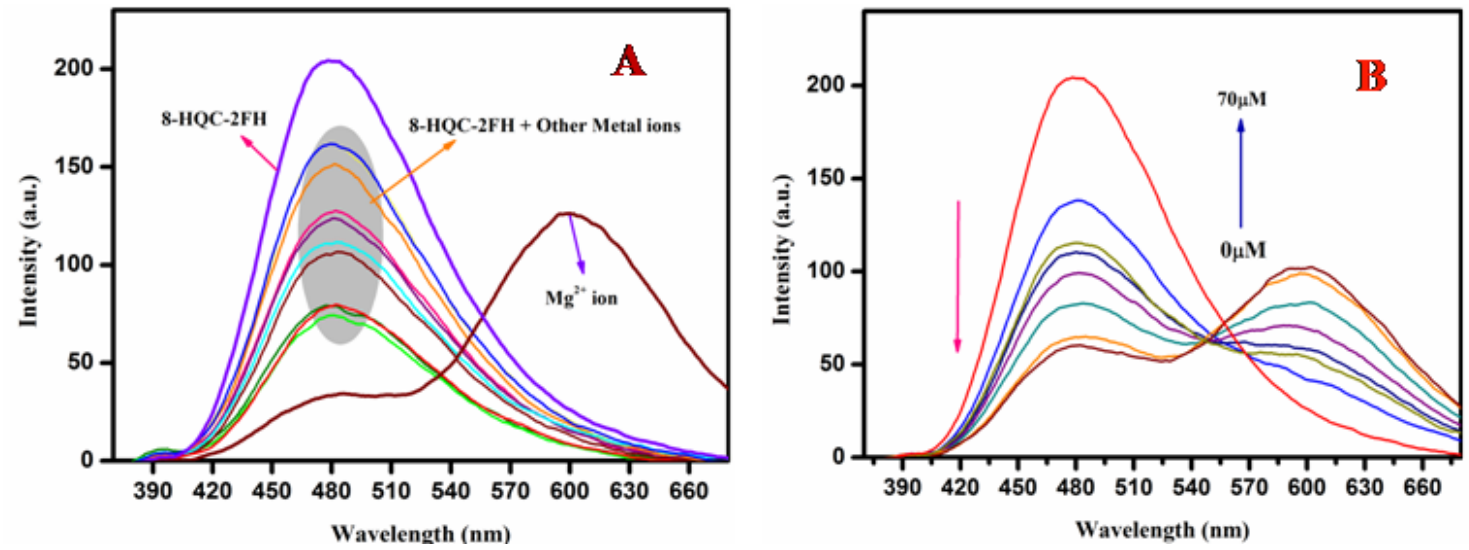

Figure 2

Figure 7A. Fluorescence spectra of 8-HQC-2TCH (25 µM) in the presence of various metal ions such as K^{+}, Mg^{2+}, Ba^{2+}, Cu^{2+}, Al^{3+}, Fe^{3+}, Zn^{2+}, Cd^{2+}, Hg^{2+} and Cr^{3+} , λ_{ex}370nm (25 µM) in DMSO**. B)** Fluorescence spectra of 8-HQC-2TCH (25 µM) upon the titration of Mg^{2+} (0 to 70 mM) in DMSO.

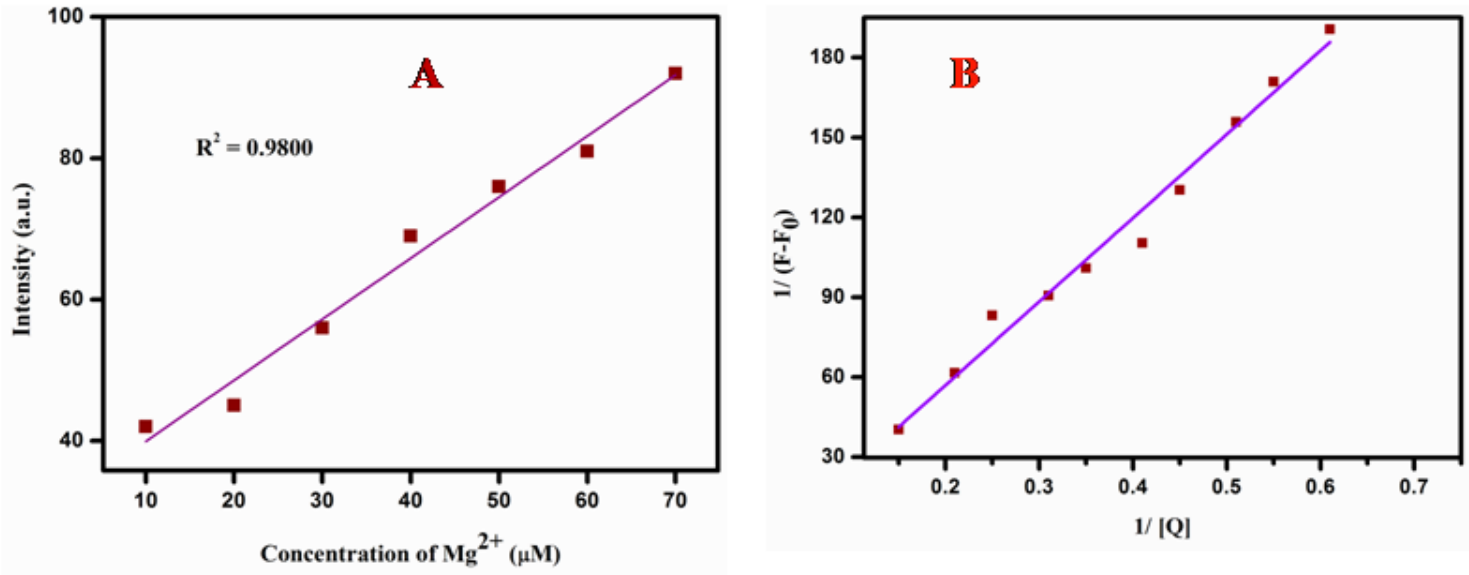

Figure 3

Figure 8A. Linear relationship plot obtained from fluorescence titration of 8-HQC-2TCH (mM) with a concentration of Mg^{2+} ions (0 to 70 mM.). **Figure B.** Benesi-Hildebrand plot, determination of the Binding constant for 8-HQC-2TCH with Mg^{2+} ion.

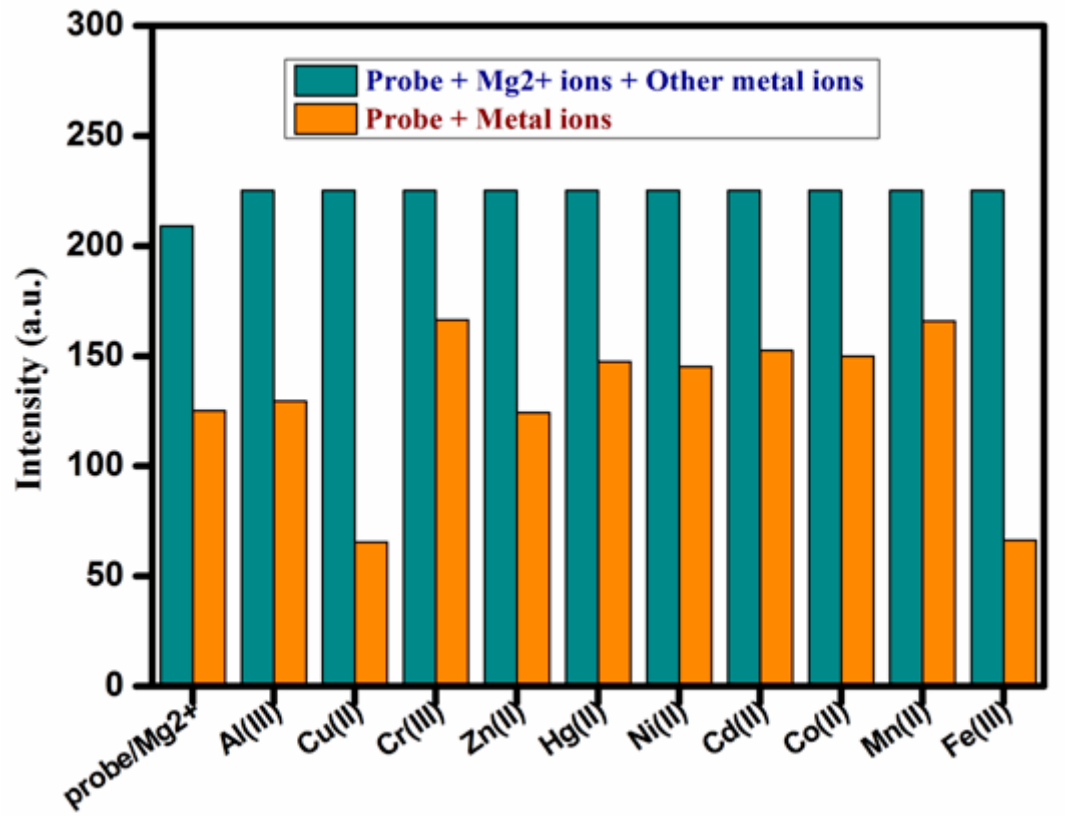

Figure 4

Figure 9. Competitive experiments of 8- HQC-2TCH toward Mg^{2+}: Cyan bars represent of various metal ions with an added into an 8-HQC-2TCH + Mg^{2+} in DMSO solution and Orange bars represent fluorescence intensity of 8-HQC-2TCH + Metal ions, λ_{ex}370nm (25μM).

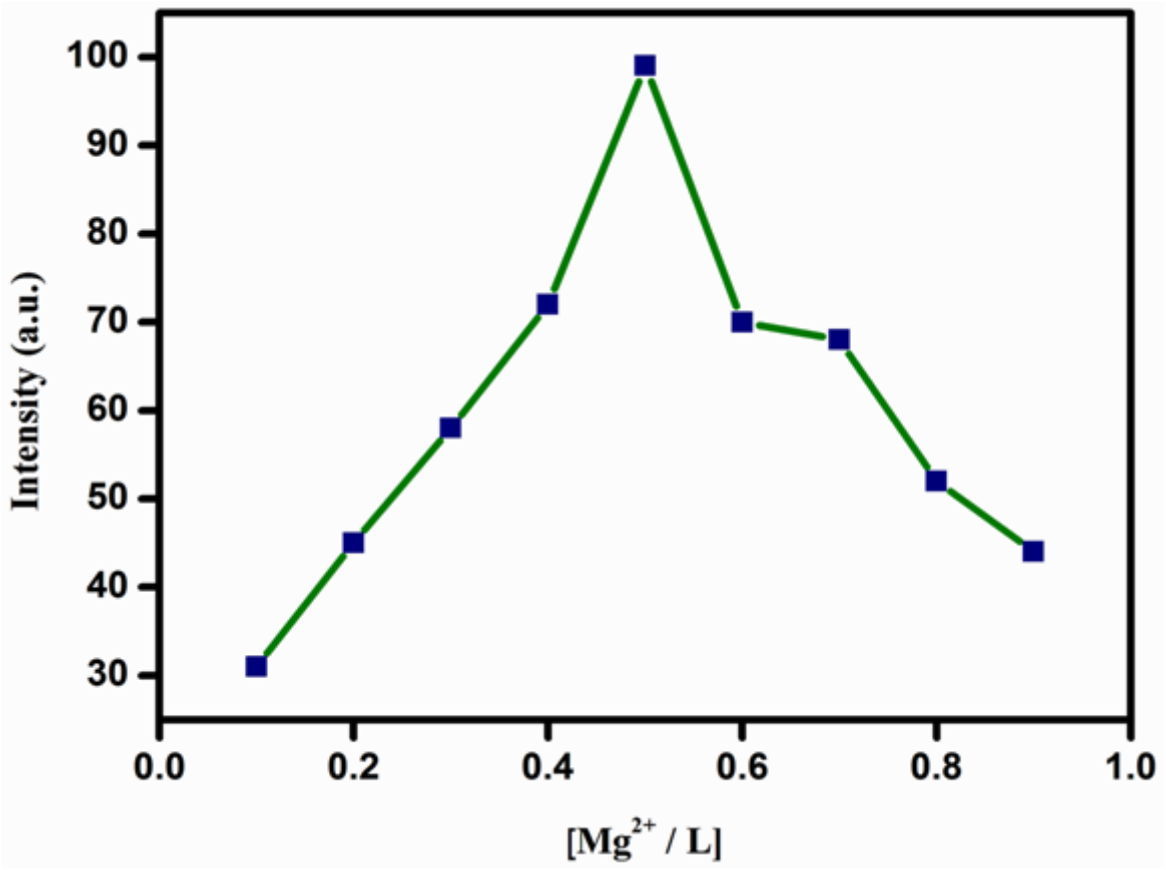

Figure 5

Figure 10. Job's plot Fluorescence intensity of diagram between 8- HQC-2TCH and Mg^{2+} ion.

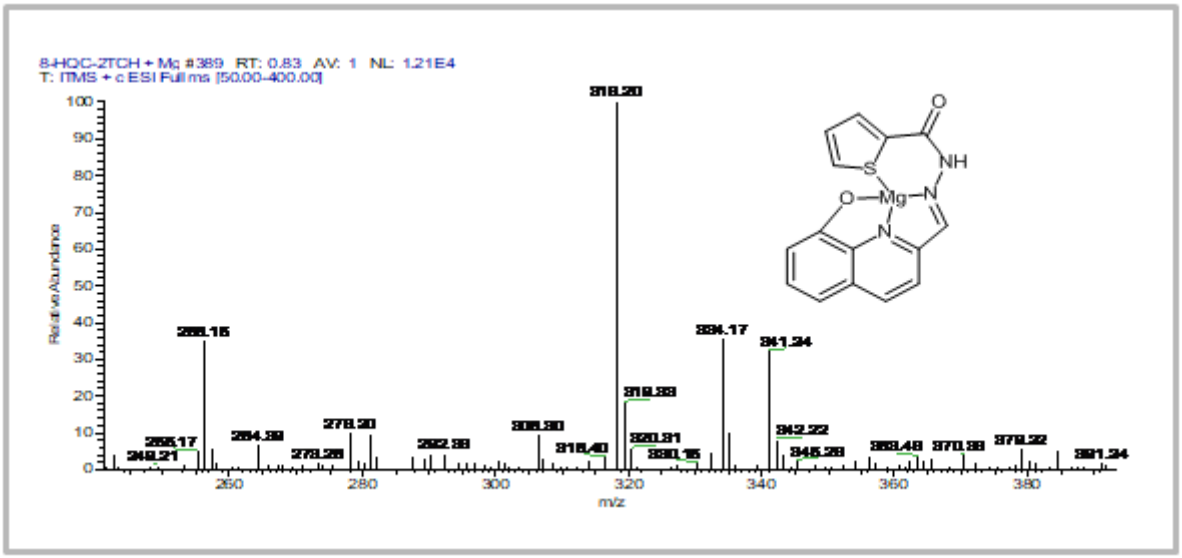

Figure 6

Figure 11. Mass Spectrum of 8- HQC-2TCH + Mg^{2+} ion.

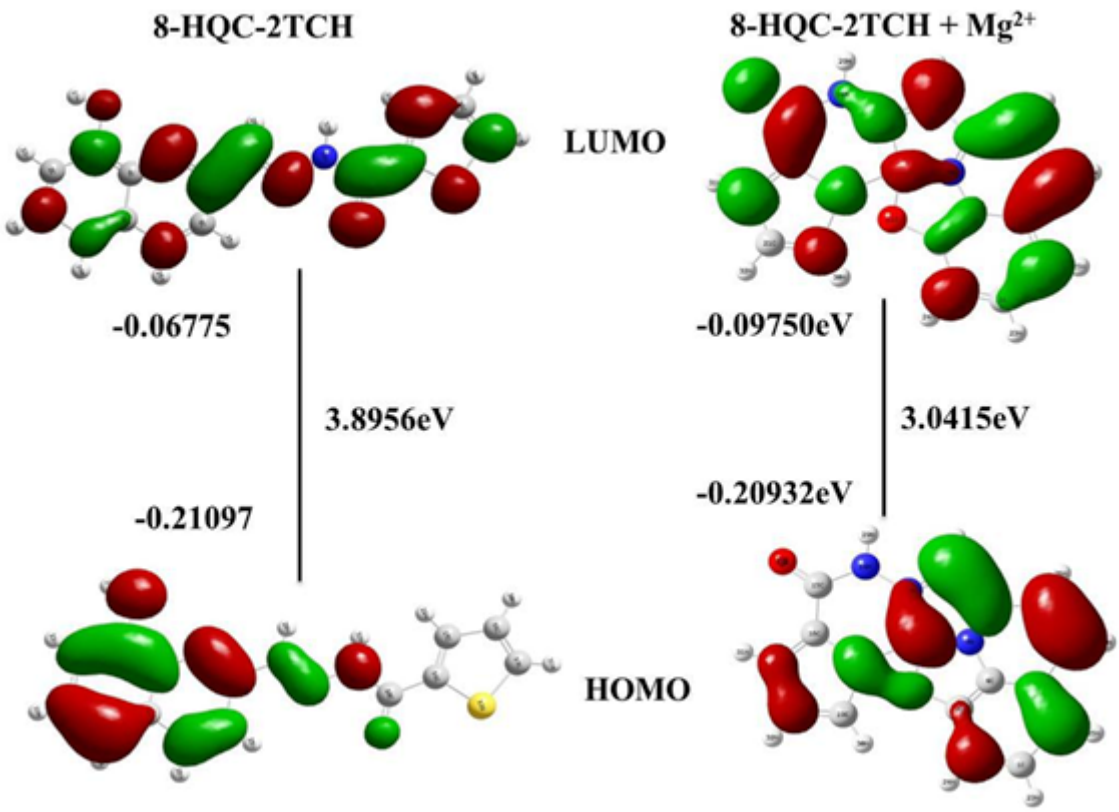

Figure 7

Figure 12. HOMO and LUMO of probe (8-HQC-NH) calculated with DFT/TD-DFT at B3LYP/6-31G (d) level using Gaussian 09.

Supplementary Files

This is a list of supplementary files associated with this preprint. Click to download.

- RevisedSupplementaryData.docx
- GraphicalAbstract.jpg
- Scheme02.png